

Hyperfine interactions at lanthanide impurities in Fe

D. Torumba,¹ S. Cottenier,^{1,*} V. Vanhoof,¹ and M. Rots¹

¹*Instituut voor Kern- en Stralingsfysica, Katholieke Universiteit Leuven, Celestijnenlaan 200 D, B-3001 Leuven, Belgium*

(Dated: October 6, 2018)

The magnetic hyperfine field and electric-field gradient at isolated lanthanide impurities in an Fe host lattice are calculated from first principles, allowing for the first time a qualitative and quantitative understanding of an experimental data set collected over the past 40 years. It is demonstrated that the common Local Density Approximation leads to quantitatively and qualitatively wrong results, while the LDA+U method performs much better. In order to avoid pitfalls inherent to the LDA+U method, a careful strategy had to be used, which will be described in detail. The lanthanide 4f spin moment is found to couple antiferromagnetically to the magnetization of the Fe lattice, in agreement with the model of Campbell and Brooks. There is strong evidence for a delocalization-localization transition that is shifted from Ce to at least Pr and maybe further up to Sm. This shift is interpreted in terms of the effective pressure felt by lanthanides in Fe. Implications for resolving ambiguities in the determination of delocalization in pure lanthanide metals under pressure are discussed. For the localized lanthanides, Yb is shown to be divalent in this host lattice, while all others are trivalent (including Eu, the case of Tm is undecided). The completely filled and well-bound 5p shell of the lanthanides is shown to have a major and unexpected influence on the dipolar hyperfine field and on the electric-field gradient, a feature that can be explained by their $1/r^3$ dependence. An extrapolation to actinides suggests that the same is true for the actinide 6p shell. The case of free lanthanide atoms is discussed as well.

PACS numbers: 71.20.Eh, 75.20.Hr, 75.25.+z, 76.80.+y, 76.60.-k

I. INTRODUCTION

A prototype problem in the field of nuclear condensed matter physics is to determine and understand the magnetic hyperfine field (HFF) at any of the elements of the periodic table, incorporated as a substitutional impurity in a simple ferromagnetic host such as bcc Fe. Understanding hyperfine fields forms a critical test for our understanding of condensed matter. Moreover, they provide a convenient tool for nuclear physicists to determine nuclear magnetic moments: two features that explain the decades of experimental¹ and theoretical^{2,3} efforts that have been devoted to this problem. Today, the hyperfine fields of all elements as substitutional impurities in bcc Fe are well-understood up to about $Z=55$ ^{4,5,6,7,8}. For the heavier 5d impurities, sizeable deviations between theory and experiment remain⁹. The hyperfine fields of very light impurities at interstitial sites in Fe have been calculated as well^{10,11}. Lanthanide impurities in Fe are much less understood, both experimentally and theoretically. As far as experiment is concerned, it is hard to obtain *reliable* values for the lanthanide hyperfine fields (and also for their electric-field gradients, see below). This problem is illustrated by the rather desperate conclusion of L. Niesen in a still useful review¹² back in 1976: “(...) *if we cannot perform experiments that yield unambiguous results, we should better do no experiments at all.*” On the theoretical side, no *ab initio* studies have been performed yet for lanthanide impurities in Fe (an approach using a model Hamiltonian is developed in Ref. 13). The reason for this lies in a known failure of the widely used Local Density Approximation (LDA) within Density Functional Theory (DFT): LDA is not suitable to describe

strong electron correlations^{14,15,16,17}. As a result, the strongly correlated and mainly *localized* 4f states in lanthanides are rendered *itinerant* by LDA. It can therefore be anticipated that for a lanthanide impurity in bcc Fe, LDA is incapable to describe correctly the interaction between these localized and strongly correlated 4f electrons and the itinerant 3d states of the host material. This could be overcome by treating the 4f states as core states, an approach that has been used in the past with some success for lanthanides^{14,15,17}. In this way, however, one forces the f-electrons to behave exactly as in free atoms, which is not entirely correct. An efficient and popular way to improve on the LDA failure without resorting to fully atomic 4f behavior, is to use the LDA+U method^{18,19,20,21,22}. In LDA+U, the correlation absent in LDA is reintroduced by an on-site Coulomb repulsion parameter U, to which an *a priori* value has to be assigned. The LDA+U method has been used in the recent past with considerable success (recent examples are Refs. 21,23,24,25,26 and many others), but it is not yet clear where the boundaries of its range of applicability are. In this work, we will examine how well LDA+U performs on a delicate quantity as the HFF.

An extra feature for lanthanide impurities in Fe that is absent for lighter impurities, is the presence of a large electric-field gradient (EFG) at the lanthanide nucleus. At a site with cubic point symmetry – such as a substitutional site in bcc Fe – the EFG tensor must be necessarily zero. Due to the strong spin-orbit coupling for these heavy impurities, however, the crystalline cubic point symmetry at the lanthanide site is lowered to a tetragonal one. This allows the existence of a large EFG at the nucleus of the impurity. The same happens for 5d impurities in Fe^{27,28,29}, but there the EFG is 2 orders

of magnitude smaller. We have calculated and analyzed this EFG for lanthanides, and compare it with the sparse experimental data.

The goals of this work can be summarized as follows. On the physical side, we want to obtain better *quantitative* and *qualitative* insight in magnetic hyperfine fields and electric-field gradients of lanthanide impurities in Fe. This should allow us to assess better the reliability of the existing experiments, and to derive the underlying physical mechanism. On the technical side, we want to examine whether the range of applicability of the LDA+U method can be extended to problems as delicate and sensitive as magnetic and electric hyperfine interactions of heavy impurities in a transition metal host. It will be shown that in the course of this analysis unexpected new results and questions show up, such as the influence of the lanthanide 5p electrons (Sec. III C and IV B) and the position of the delocalization-localization transition in this system (Sec. III C and V A).

II. COMPUTATIONAL DETAILS

All our calculations were performed within Density Functional Theory^{30,31,32}, using the Augmented Plane Waves + local orbitals (APW+lo) method^{32,33,34} as implemented in the WIEN2k package³⁵ to solve the scalar-relativistic Kohn-Sham equations. In the APW+lo method, the wave functions are expanded in spherical harmonics inside nonoverlapping atomic spheres of radius R_{MT} , and in plane waves in the remaining space of the unit cell (=the interstitial region). For the Fe atoms a R_{MT} value of 2.20 a.u. was chosen, while for the lanthanide impurity we used $R_{\text{MT}}=2.45$ a.u. The maximum ℓ for the expansion of the wave function in spherical harmonics inside the spheres was taken to be $\ell_{\text{max}} = 10$. The plane wave expansion of the wave function in the interstitial region was made up to $K_{\text{max}} = 7.5/R_{\text{MT}}^{\text{min}} = 3.41$ a.u.⁻¹, and the charge density was Fourier expanded up to $G_{\text{max}} = 16\sqrt{Ry}$.

The lattice constant of Fe was fixed at the experimental value of 2.87 Å. In order to reproduce the situation of an isolated impurity in bulk Fe, we used the supercell approach with a $2 \times 2 \times 2$ supercell where one iron atom was replaced by a lanthanide atom. The neighboring Fe atoms will be displaced by the presence of this impurity, as was documented before for lighter impurities in Fe^{3,7,8}. We took this effect into account in an average way by relaxing the nearest neighbors for Eu as an impurity (which is in the middle of the lanthanide series), and kept the same relaxation fixed for all other lanthanides. The Eu-Fe distance was 2.60 Å which is an increase of 0.11 Å with respect to the Fe-Fe distance and which is almost identical to the distance between 5p impurities and their Fe neighbors⁸. It was tested for another lanthanide (Er) that there was only a marginal difference of less than 1 T between the HFF obtained with the Eu-Fe distance and the correct Er-Fe distance (2.58 Å). A test

for an extended supercell of 32 atoms was also performed. We relaxed the first four nearest neighbors. The Eu-Fe distance hardly changed (2.63 Å) and the Fermi contribution to the hyperfine field changed with 5 T. For the sampling of the Brillouin zone (BZ) of the $2 \times 2 \times 2$ supercell we took 75 special k-points in the irreducible part of the BZ, which corresponds to a $10 \times 10 \times 10$ mesh.

As exchange-correlation functional, the Local Density Approximation (LDA)³⁶ was used. Spin-orbit (SO) coupling was taken into account in all the calculations by a second-variational step scheme³⁷, using a cut-off energy $E_{\text{cut}}^{\text{SO}} = 3.0$ Ry. Relativistic Local Orbitals (RLO) for the lanthanide 5p states were added to the basis set, because it is known that for actinides this allows to reduce the basis set size needed for the second variational step³⁸ (=lower $E_{\text{cut}}^{\text{SO}}$). Limitations in the implementation prevent to obtain correct EFG's and dipolar HFF's when RLO's are used. Therefore, whenever such information was needed, the calculations were repeated without RLO's. This never had a large influence on the obtained values, however. For the LDA+U method, the 'Around the Mean Field' (AMF) scheme of Czyżyk and Sawatzky¹⁹ was used. The choice of the U and J parameters is discussed in detail in Sec. III C.

Free atoms were simulated by a supercell containing only one lanthanide and vacuum otherwise, leading to a separation of 9.4 Å between two 'neighboring' lanthanides. For free ion calculations, this cell was charged. All the other parameters were chosen exactly the same as in the calculations for lanthanides in Fe.

III. MAGNETIC HYPERFINE FIELDS

A. Experimental data set

Let us first have a look at the experimental data set for the HFF (Fig 1-a). Only in 4 cases the magnitude of the HFF *and* its sign are known with high reliability (the sign of the HFF indicates whether the field is parallel (+) or antiparallel (-) with respect to the magnetization of the Fe host lattice). These cases are La (-47(1) T)³⁹, Ce (-41(2) T)⁴⁰ and Lu (-73.12(36) T)⁴¹ for which Nuclear Magnetic Resonance on Oriented Nuclei (NMR/ON) has been performed, and Yb (-125(8) T)⁴² on which Time-Dependent Perturbed Angular Correlation spectroscopy (TDPAC) has been applied. The latter technique has also been used for Gd⁴³, albeit on a recoil-implanted sample which is not necessarily clean. The value of -26(8) T obtained in this way agrees well with an in principle reliable Mössbauer measurement of -37 T, which is unfortunately not very well documented⁴⁴. Three time-integrated Perturbed Angular Correlation (IPAC) measurements are available for Gd as well – IPAC is a method that is rather unreliable, and can merely be used to determine the sign and an order of magnitude. They yield -20(5) T⁴⁵, -18(9) T⁴⁶ and -7 T⁴⁷. A HFF of -30(10) T can therefore be assigned to Gd in Fe in a reli-

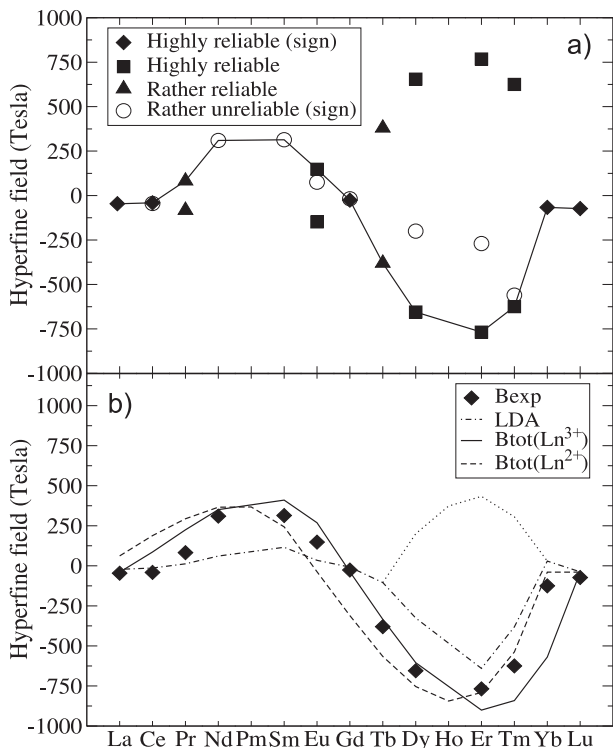


FIG. 1: a) Experimental data set for the magnetic hyperfine fields of lanthanides in Fe. If the sign of the HFF is not measured, the data point is plotted both at positive and negative values. Distinction is made between highly reliable data for which the sign is measured (diamond), highly reliable data without sign measurement (square), less reliable data without sign (triangle) and data that are rather unreliable for the magnitude of the HFF but reliable for the sign (circle). For references and values, see text. The line connects the most likely values for all lanthanides. If multiple measurements with the same reliability were available, only one of them is given. More data can be found in the compilation of Rao¹. b) Comparison between experiment and several types of calculations for the magnetic hyperfine field of lanthanides in Fe. Diamonds: most probable experimental data points (this is the full line from Fig. 1-a). Dotted-dashed line: LDA results for the antiferromagnetic orientation (Campbell-Brooks orientation). Dotted line: LDA results for the ferromagnetic orientation when this one has the lowest energy. Full line: LDA+U value for trivalent lanthanides. Dashed line: LDA+U value for divalent lanthanides.

able way. In 4 other cases the magnitude of the HFF but not its sign has been measured with an accurate method as Mössbauer Spectroscopy (MS): Eu (148.2(9) T)^{48,49}, Dy (610(7) T)⁵⁰, Er (768(13) T)⁵¹ and Tm (671 T)¹². For Pr⁵² and Tb⁵³, the magnitude but not the sign has been measured with Low Temperature Nuclear Orientation (LTNO). This non-resonant technique provides data that are less accurate than the previous ones, although they still are reasonably reliable. Finally, in the case of Ce⁵⁴, Nd⁴⁵, Sm⁵⁵, Eu⁴⁵, Gd⁴⁶, Dy⁴⁶, Er⁵⁶ and Tm⁵⁷ IPAC experiments have been reported, from which only

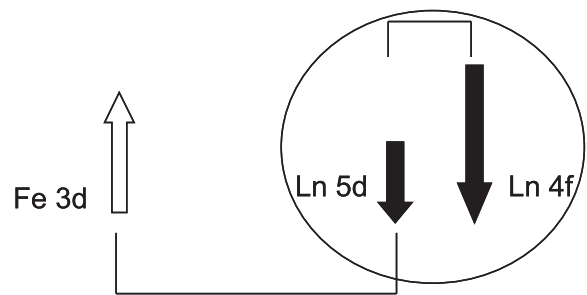


FIG. 2: Schematic summary of the model of Campbell and Brooks. The localized 4f spin moment does not interact directly with the moments of neighboring atoms. But it does interact with the 5d moment on the same atom by ferromagnetic intra-atomic exchange. The more delocalized 5d spin moment interacts by antiferromagnetic interatomic exchange with the Fe 3d moment. As a result, the net interaction between Fe-3d and lanthanide-4f is antiferromagnetic. A consequence of the model of Campbell and Brooks is the positive (negative) HFF in the first (second) half of the lanthanide-series in Fe (Fig. 1-a). Due to Hund's third rule, the lanthanide 4f orbital moment is antiparallel (parallel) to the 4f spin moment in the first (second) half of the series. Because the orbital contribution to the HFF (which is parallel to the orbital moment) is dominant for lanthanides, the total HFF is parallel (antiparallel) to the Fe moment – and hence called positive (negative) – in the first (second) half of the series.

the sign information can be reasonably trusted (see e.g. the agreement with other experiments in Fig. 1-a and Ref. 1). Due to the the latter sign information, the HFF of the light lanthanides is guessed to be positive, while for the heavy lanthanides it is negative. The line in Fig. 1-a summarizes the most likely interpretation of this data set.

Fig.1-a can be understood in terms of Hund's rules and the model of Campbell and Brooks. Based on heuristic arguments (Ref. 58) and first principles calculations (Ref. 59), Campbell and Brooks showed that the *inter-atomic* exchange interaction between a transition metal 3d spin moment and a lanthanide 5d spin moment is antiferromagnetic (Fig. 2). The lanthanide 4f moment is localized at the lanthanide site and cannot directly interact with its transition metal neighbors, but it has a ferromagnetic *intra-atomic* exchange interaction with the lanthanide 5d moment. The result is a net antiferromagnetic coupling between the lanthanide 4f moment and the transition metal 3d moment (Fig. 2). According to Hund's third rule, the lanthanide orbital moment is antiparallel to the lanthanide spin moment for the 7 lightest lanthanides, and parallel to it for the 7 heaviest lanthanides. The dominant contribution to the HFF is the orbital HFF (see Sec. III B and Fig. 3), which is parallel to the orbital moment. Therefore, one expects the total HFF to be parallel to the Fe magnetization (and hence positive) for the light lanthanides, and antiparallel (negative) for the heavy ones, as is seen indeed in Fig. 1-a.

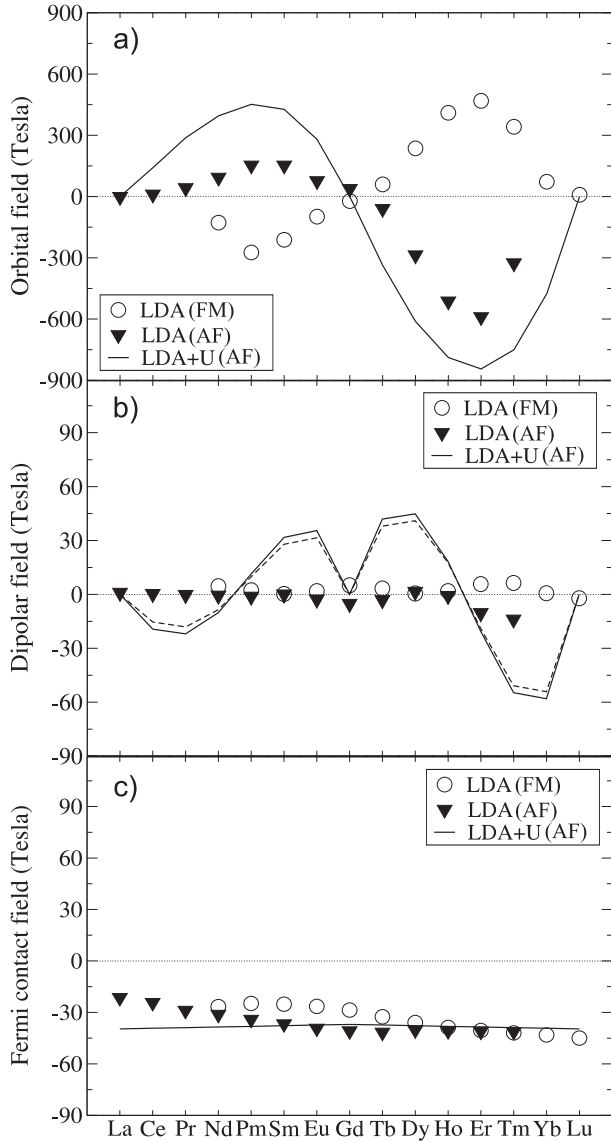


FIG. 3: White circles indicate the ferromagnetic solution (FM), black triangles the antiferromagnetic solution (AF). Symbols are LDA results, lines are LDA+U results (obtained from Hund’s rules occupations, see text). Mind the scale, which is 10 times larger in a) compared to b) and c). a) Orbital contribution to the HFF at the lanthanide site due to 4f electrons. b) Dipolar contribution due to 4f only (fully line), and due to 4f and 5p (dashed line, see text). c) Fermi contribution. The total HFF is the sum of these 3, and is almost undistinguishable from a).

B. LDA calculations

As a first step, we calculate the magnetic HFF with the common LDA. This will provide us with a data set to which we can later compare the possible improvement by LDA+U, and it allows to introduce some peculiarities that will play a role in all later calculations as well. As is usual with this type of methods, our calculations involve

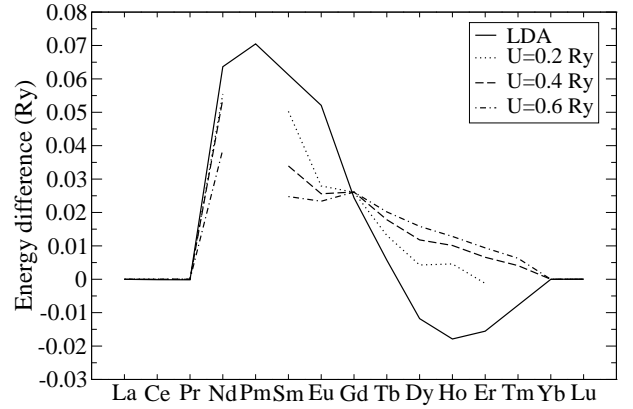


FIG. 4: Energy difference between the situations with the lanthanide 4f spin moment ferromagnetically aligned with the Fe 3d moment and with the 4f moment antiferromagnetically aligned ($E_{\text{FM}} - E_{\text{AF}}$). If this energy difference is positive, the antiferromagnetic situation has the lowest energy. Energy difference for LDA are compared with energy differences for LDA+U with progressively larger U. The LDA result is equivalent to $U=0.0$ Ry. There are some gaps in the picture, because not for every situation a converged solution could be found. For Pm the calculated energy difference is much larger (0.42 Ry for $U=0.6$ Ry) and is out of scale.

an iterative procedure (‘self-consistent field’ procedure) that yields in the end a possible state of the calculated system, which is not necessarily the desired ground state: in the space of possible solutions, this self-consistent field procedure finds a *local* minimum, but not necessarily the *global* minimum. The local minimum that is obtained, depends to some degree on the starting configuration that was initially chosen. This behavior is prominently present for lanthanides in Fe. If the spin moment of the lanthanide initially is put parallel to the Fe spin moment, then this parallelism is maintained throughout the iterative procedure (except for La, Ce and Pr, where the moment always spontaneously turns to an antiparallel orientation). We call this from now on the ferromagnetic solution. With an initially antiparallel configuration, an antiparallel (or antiferromagnetic) solution is obtained. If the lanthanide was given initially no spin moment, then a solution with a spin moment that is much reduced compared to the two preceding solutions was found. In order to decide which of those is the ground state, one has to look at the total energy of each solution. The total energy of the case with reduced moment was much higher than the others, and we will not consider it further. The energy differences between the other two solutions are given in Fig. 4. For all lanthanides up to Tb, the antiferromagnetic solution has the lower energy. Starting with Dy, the ferromagnetic solution becomes the ground state.

In Fig. 3, the different contributions to the magnetic HFF are given for both types of solutions. A HFF is a magnetic field at the position of the nucleus, and it

is built mainly from 3 contributions: the spin dipolar field, the Fermi contact field and the orbital field. The spin dipolar field is generated by the spin moments of the electrons surrounding the nucleus. For cubic point symmetry, this contribution vanishes. The Fermi contact field⁶⁰ is of dipolar nature as well, but is due to the penetration of s-electrons into the nucleus. It does not vanish for cubic symmetry, and it is the dominant (and almost only) contribution for impurities up to $Z=55$ in Fe. The orbital field stems from the electric charge of the electron that orbits the nucleus, and it vanishes for cubic symmetry. As Fig. 3 shows, the dipolar field does not exceed a few Tesla, while the Fermi contact field lies between -20 T and -40 T. The orbital field is the dominant contribution, and can reach almost ± 600 T. At first sight, one would expect a zero orbital and dipolar field for a substitutional impurity in Fe, as the point symmetry is cubic. The reason why this is not the case for lanthanides, is purely due to the presence of spin-orbit coupling, which breaks the crystalline cubic point group symmetry. The oscillatory behavior of the orbital moment reflects Hund's third rule: the orbital moment is antiparallel (parallel) to the spin moment in the first (second) half of the lanthanide series. Because the orbital field is parallel to the orbital moment, it will for the antiferromagnetic solution be positive in the first half of the series and negative in the second half (and vice versa for the ferromagnetic solution).

According to the LDA total energies, we have to accept the antiferromagnetic solution as the ground state up to Tb, and the ferromagnetic solution starting from Dy. This leads to positive HFF's for almost all lanthanides (Fig. 1-b), which is contradiction with the current interpretation of the experimental data set and with the model of Campbell and Brooks. We will demonstrate in Sec. III C that this is a new, clear example of a failure of LDA, to be added to the list of notorious shortcomings as the general overbinding behavior, the prediction of the wrong crystal structure for Fe, and the prediction of metallicity for some strongly correlated insulators as NiO and La_2CuO_4 . Even if we would select the antiferromagnetic solution throughout (as the Campbell-Brooks model suggests), then still the quantitative agreement with the experimental HFF's is rather poor (Fig. 1-b).

C. LDA+U calculations

Using and interpreting LDA+U calculations brings some complications that are absent for LDA. First, LDA+U schemes are not fully *ab initio*: they involve an on-site Coulomb repulsion parameter U and an on-site exchange interaction constant J that have to be chosen *a priori* for every atom with strong correlations. In our case we have to choose one U and one J for the f-states of the lanthanide impurity. In line with the strategy adopted for the relaxation (Sec. II), we strive for reasonable overall agreement and do not focus on agree-

ment for individual cases too much. Therefore we take the same U and J for all lanthanides. Looking at other calculations^{18,61} and experiments^{62,63}, $U = 0.6$ Ry is a reasonable choice. The value of J is usually an order of magnitude smaller, and it does not affect the results as much as U does. Therefore we take J as 10% of U . Another – second – complication with LDA+U is that due to the introduction of tuneable variables U and J , the total energy loses its exact mathematical meaning as a variational quantity. If LDA+U is used, a lower energy for one solution does therefore not necessarily mean that this solution is to be preferred over another one with a higher energy. This does not mean that these total energies are meaningless: for instance, LDA+U has been used successfully to determine the equilibrium volume of materials by energy minimization⁶⁴. The current general opinion is that if the electronic structure does not *qualitatively* change between two slightly different situations, then the total energies obtained by LDA+U for these situations can probably be compared. The criterion to decide whether there is a qualitative difference between two electronic structures or not, is provided by the 4f density matrix: in qualitatively similar cases, the occupation of the 14 m-orbitals (= the diagonal elements of the two spin-polarized 7×7 density matrices) should be more or less identical. Finally – and third – there are much more local minima in the space of solutions when LDA+U is used, and a calculation gets easily trapped in one of them. Because the density matrices for two different solutions are necessarily different from each other, the total energy cannot be used to determine which solution is the ground state. This problem is illustrated in Tab. I, where the diagonal elements of the f-up density matrix is given for various antiferromagnetic solutions for Tm in Fe. The 5 electrons can be distributed in different ways over the 7 orbitals, and always a converged solution can be obtained. The HFF field can be very different for all cases. In the second column, the total energy of these 5 solutions is given, relative to the case with the lowest energy (case 2). Case 1 – which we will later identify as the most probable ground state – is only third in rank if the total energy is considered: an illustration of the lack of meaning of the LDA+U total energy for cases with different density matrices. This makes it impossible to proceed in a straightforward way as was done for LDA.

Faced with this problem, we first take one step back and examine the energy difference between the ferromagnetic and the antiferromagnetic case *for the same type of solution* (i.e. for a ferro- and antiferromagnetic solution that have a similar f-electron density matrix). These energy differences can be expected to be meaningful (see above), a hope which is supported by the fact that we find them not to depend on the type of solution for which we make the comparison. The result is shown in Fig. 4, for 3 different values of U : 0.2, 0.4 and 0.6 Ry (some gaps are present, because not for every lanthanide a solution could be found for every U). Clearly, the use of a non-zero U makes the antiferromagnetic case more

TABLE I: Diagonal elements of the 7×7 4f-up density matrix for Tm in Fe (antiferromagnetic case), together with the orbital (4f), dipolar (4f+5p) and Fermi contributions to the total HFF (Tesla). These diagonal elements give the occupation of each m-orbital (between 0 and 1). The LDA result is compared with several LDA+U calculations, all with $U=0.6$ Ry. The LDA+U calculations differ only in the initial distribution of the f-electrons over the different orbitals. In the second column, the total energy (in mRy/atom) of the LDA+U calculations is given, relative to case 2, which has the lowest energy (see text for discussion).

	ΔE	m=-3	m=-2	m=-1	m=0	m=1	m=2	m=3	B_{orb}	B_{dip}	B_{Fermi}	B_{tot}
LDA		0.98	0.95	0.96	0.71	0.86	0.52	0.54	-326	-14	-41	-381
case 1	1.7	1.00	0.99	0.99	0.99	0.99	0.01	0.01	-718	-63	-41	-822
case 2	0.0	0.99	0.99	0.99	0.99	0.01	0.99	0.01	-571	-27	-41	-639
case 3	1.6	0.99	0.99	0.99	0.02	0.99	0.99	0.01	-425	-16	-42	-483
case 4	3.2	0.99	0.99	0.02	0.99	0.99	0.99	0.01	-275	-28	-42	-345
case 5	8.9	1.00	0.04	0.99	0.99	0.99	0.99	0.01	-126	-63	-42	-231

stable, for all lanthanides. This brings the sign of the HFF in agreement with experiment and with the model of Campbell and Brooks. We conclude that LDA+U describes the effective d-f exchange interaction much better than LDA does, and that LDA is qualitatively wrong in this respect.

Next, we try to find a way to obtain ground state values for the HFF in the antiferromagnetic case. To this end, we turn the annoying freedom of having several ways to occupy the m-orbitals into an advantage, by determining the *individual contribution* of each m-orbital to e.g. the orbital field. This can be done by first calculating the orbital HFF for several different antiferromagnetic solutions, as is given as an example for Tm in Tab. I. Then a system of linear equations is set up, with as 7 variables x_m the orbital HFF of each of the 7 m-orbitals. The occupation of each of these orbitals (or the diagonal elements of the density matrix from Tab. I) are the coefficients. The occupation found in the calculation should give the calculated orbital field, as is illustrated here for ‘case 1’ in Tab. I:

$$1.00x_{-3} + 0.99x_{-2} + 0.99x_{-1} + 0.99x_0 + 0.99x_1 + 0.01x_2 + 0.01x_3 = -718$$

This system of equations can be supplemented by other equations expressing some general truths (the orbital field with all 7 m-orbitals filled is zero, the contribution by +m is opposite to the one by -m), such that the system becomes overdetermined. Each subset of 7 independent equations should give the same x_m , which indeed they do.

This was done for 10 elements from the lanthanides series (Ce, Nd, Pm, Sm, Tb, Dy, Ho, Er, Tm and Yb), not only for the orbital HFF but also for the orbital moment and the dipolar HFF. The dominant contribution to the orbital HFF is due to the 4f electrons, as one could expect (Fig. 6-a,b). Orbitals with opposite m quantum number yield opposite orbital hyperfine fields. The latter can be understood as follows (see also Tab. II): in orbitals with opposite m , the electrons move in opposite directions,

TABLE II: Overview whether μ_{orb} , B_{orb} , B_{dip} and V_{zz} depend on the shape of the 4f orbital (given by the absolute value of m), the direction of motion of the electron in that orbital (given by the sign of m), and whether they depend on the charge or on the spin of the 4f electron in a given m -orbital

	μ_{orb}	B_{orb}	B_{dip}	V_{zz}
shape of orbital	yes	yes	yes	yes
direction of motion	yes	yes	no	no
charge or spin	charge	charge	spin	charge

because opposite m (z-component of the orbital angular momentum) mean that the angular momenta of those orbitals have different orientations. Hence, the orbital fields will be opposite as well. As a function of Z, the contribution due to each m-orbital increases. A linear fit is possible (full line). In order to verify whether this is accidental or not, we did the same calculations for free lanthanide atoms and free lanthanide 3^+ ions. For the free ions, almost the same perfect linear correlation was found as for the solid (dotted line in Fig. 6). For free neutral atoms, the fields were slightly larger (at most 10% for the orbital field, and 5% for the dipolar field).

Additional to this large 4f contribution, there is also a 5p contribution to the orbital HFF (Fig. 6-c-e). The up and down contributions are quite large (40-90 T), but they cancel each other, yielding a negligible (< 3 T) total contribution for the 5p-orbital HFF. This 5p-contribution to the orbital HFF does not depend on the f-configuration. Taking Dy as an example – 2 electrons in the unfilled spin channel – the total 5p orbital field will be -2 T (72 T for 5p-up, -74 T for 5p-down), irrespective whether these 2 electrons are e.g. in the $m=+3$ and $m=+2$ or in the $m=-1$ and $m=0$ orbitals. This will be different for dipolar hyperfine fields and for the electric-field gradient. Looking separately to the 5p up and down contributions, one can see that they don’t vanish for La (4f empty) and Lu (4f full), and that they increase with Z.

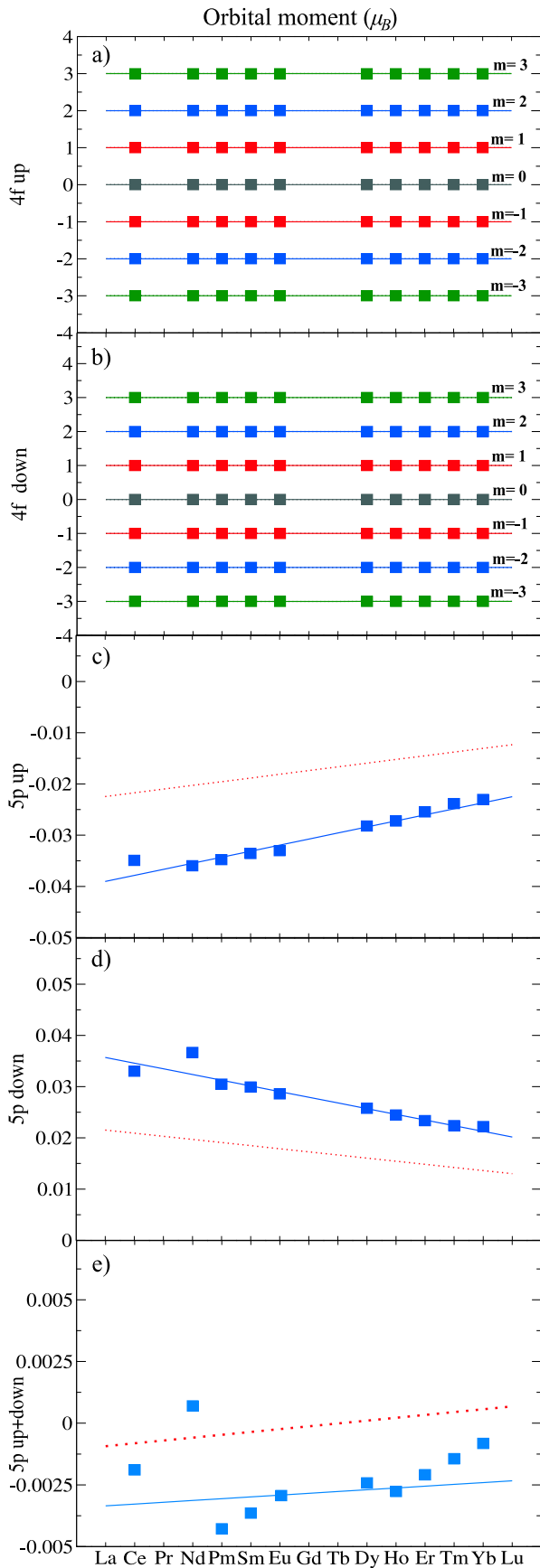


FIG. 5: Contribution of each m -orbital to the (a) 4f-up, (b) 4f-down orbital moment and the contribution of the (c) 5p-up, (d) 5p-down, (e) 5p up+down electrons to the orbital magnetic moment of a lanthanide in Fe. Data points: results from calculations for lanthanides in Fe. Full lines: linear fit through these data points. Dotted lines: linear fit through a complete set of calculations for free lanthanide ions.

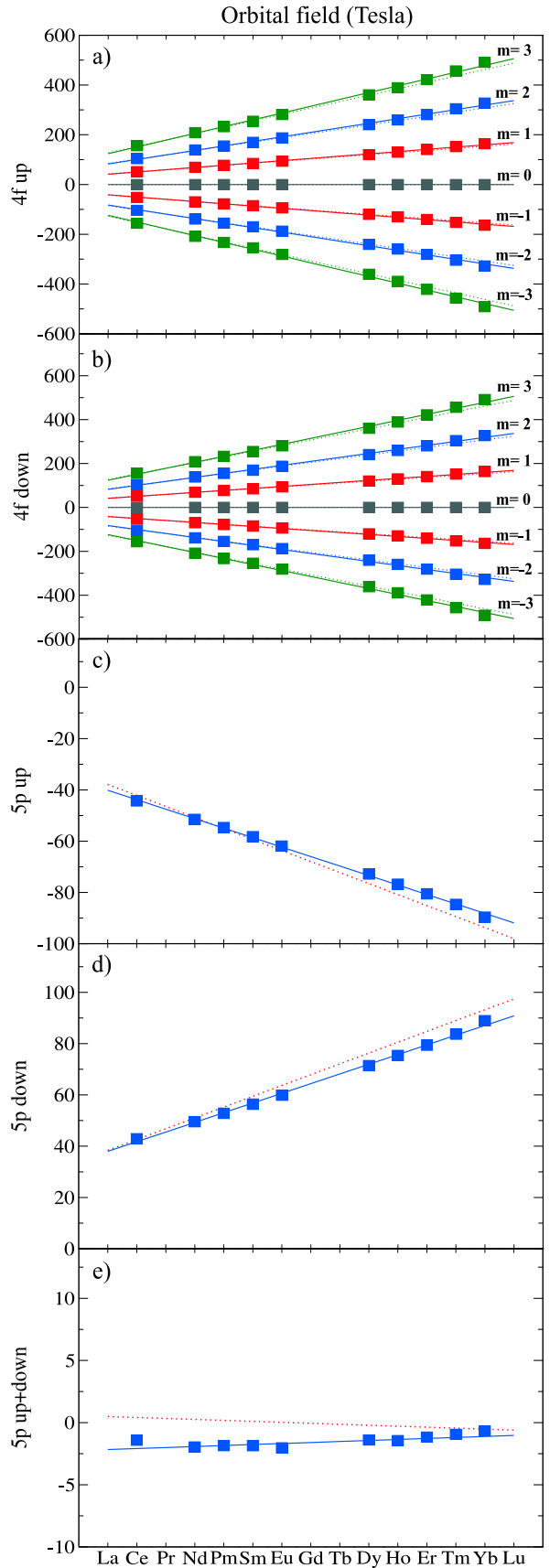


FIG. 6: Contribution of each m -orbital to the (a) 4f-up, (b) 4f-down orbital HFF and the contribution of the (c) 5p-up, (d) 5p-down, (e) 5p up+down electrons to the orbital HFF of a lanthanide in Fe. Data points: results from calculations for lanthanides in Fe. Full lines: linear fit through these data points. Dotted lines: linear fit through a complete set of calculations for free lanthanide ions.

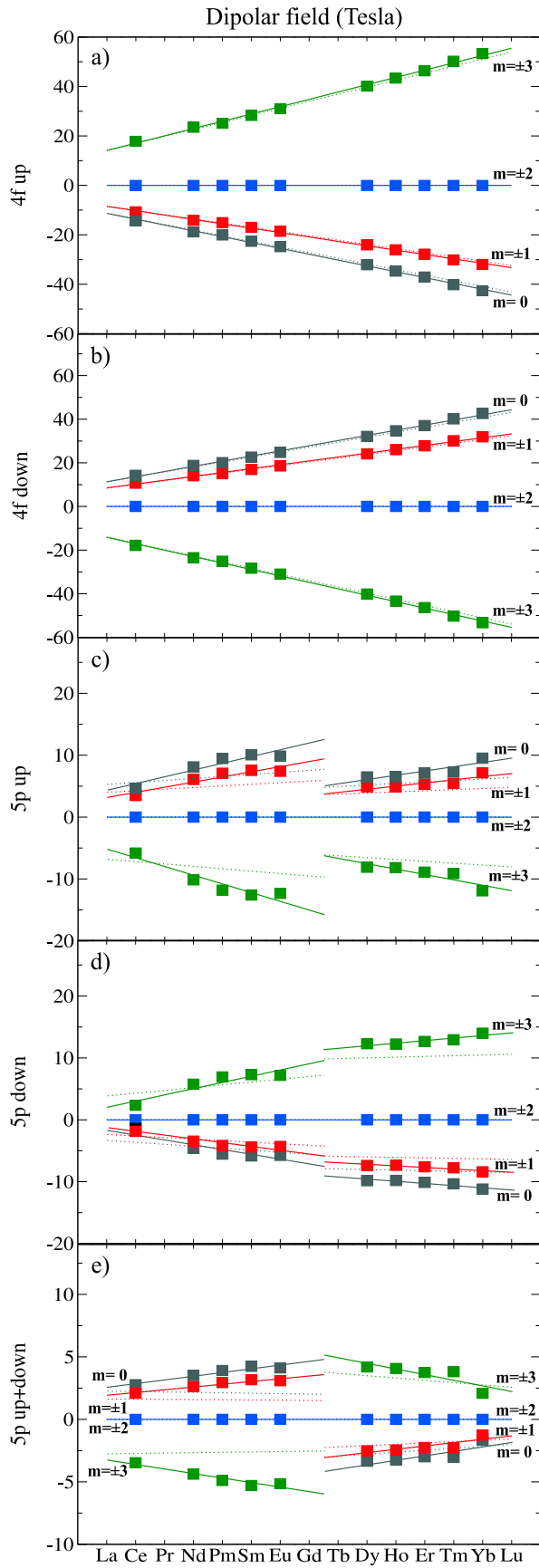


FIG. 7: Contribution of each m -orbital to the (a) 4f-up, (b) 4f-down dipolar HFF and the induced (c) 5p-up, (d) 5p-down, (e) 5p up+down contributions to the dipolar HFF of a lanthanide in Fe. Data points: results from calculations for lanthanides in Fe. Full lines: linear fit through these data points. Dotted lines: linear fit through a complete set of calculations for free lanthanide ions.

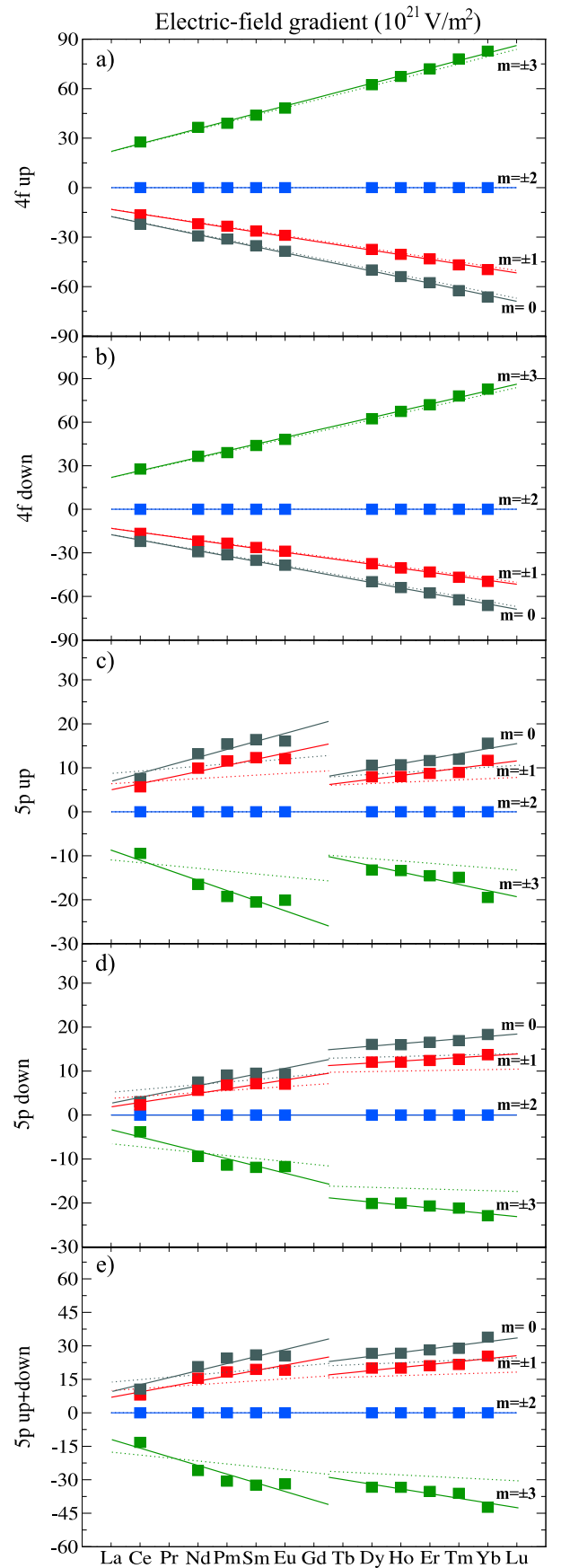


FIG. 8: Contribution of each m -orbital to the (a) 4f-up, (b) 4f-down to the total V_{zz} and the induced (c) 5p-up, (d) 5p-down, (e) 5p up+down to the total V_{zz} of a lanthanide in Fe. Data points: results from calculations for lanthanides in Fe. Full lines: linear fit through these data points. Dotted lines: linear fit through a complete set of calculations for free lanthanide ions.

Moreover, we observed that this contribution disappears if the SO-coupling is switched off. Therefore we can conclude that these 5p-contributions are due to an intrinsic p-effect, induced by the SO-coupling on the p-electrons which breaks the cubic symmetry. Finally there is also a contribution from the valence 6p-electrons, also induced by the SO-coupling, but this contribution is really small and can be neglected. The numerical stability of this analysis can be checked by repeating it for the orbital moment (Fig. 5). The contribution to the orbital moment of each m-orbital should be m by definition, which is found indeed (Fig. 5-a,b). The 5p-contributions to the orbital moment have the same origin as in the case of the orbital HFF, namely the SO-coupling.

For the dipolar HFF as well, the 4f-contribution remains the dominant one (Fig. 7-a,b), but it is one order of magnitude smaller than the orbital HFF. The systematics are different from the orbital moment and orbital HFF as well (Fig. 7-a,b and Tab. II). First of all, the dipolar HFF does not depend on the direction of motion of an electron, such that $\pm m$ -orbitals yield the same dipolar HFF. Secondly, B_{dip} depends explicitly on the electron spin, such that an electron with opposite spin in the same m -orbital yields an opposite field. Furthermore, we can observe from Fig. 7-c,d,e that the 5p-contributions to B_{dip} depend on the 4f-occupation. If we take again Dy as an example and put the 2 electrons in the +3 and +2 orbitals (spin up) we get an induced 5p-contribution of 4 T (-8 T for 5p-up and 12 T for 5p-down), while this is -3 T (4 T for 5p-up and -7 T for 5p-down) if the 2 electrons are in the +1 and -2 orbitals (spin up). Such a 4f-dependence was not present for μ_{orb} and B_{orb} . In Sec. IV B we will see that also for the EFG there is such an explicit 4f-dependence, and we will be able to explain this by the radial dependencies, which are $1/r$ for μ_{orb} and B_{orb} , and $1/r^3$ for B_{dip} and V_{zz} . Another observation from Fig. 7 is that the induced 5p-contributions behave differently in the first and the second half of the lanthanide series. This suggests a spin-dependent interaction: In the first half of the series the unfilled f-band is the down band. The 5p-up contribution is large, the 5p-down is smaller. In the second half the unfilled f-band is the up band. Now the 5p-up contribution is small and 5p-down smaller. Apparently the 4f-electrons induce a larger contribution in the 5p with opposite spin. The 6p-contribution remains negligible also for the dipolar HFF.

For the Fermi contribution, we cannot follow the procedure of Fig. 6, as this contribution is less directly connected to the occupation of the f-states. In Fig. 9, the Fermi contribution (for valence (mainly 5s and 6s) and core electrons (mainly 1s to 4s) separately) is plotted as a function of the 4f spin moment, and this for different lanthanides and different types of solutions. Both the core and valence Fermi contribution depend linearly on the 4f moment, and they sum to an almost constant value that is independent of the 4f moment. As this constant contribution is there even for a zero 4f spin moment, it must be due to other than the 4f electrons. Actually, it

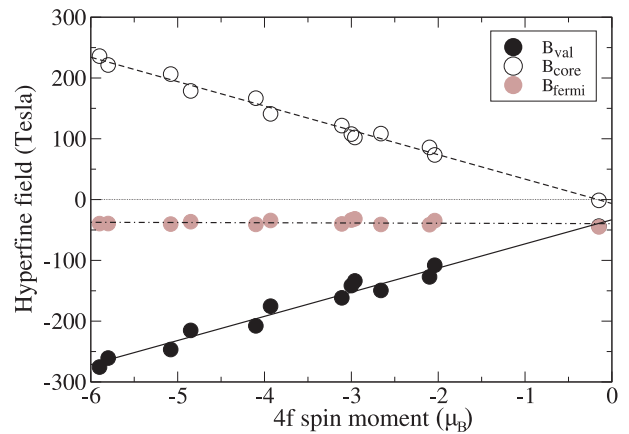


FIG. 9: Fermi contact contribution to the HFF as a function of 4f spin moment for a large set of different solutions for different lanthanides in Fe. White circles: core contribution. Black circles: valence contribution. Gray circles: total Fermi contact contribution. The lines through the core and valence contributions are linear fits, the line through the total Fermi field is the sum of those two fits.

results from the 6s-polarization due to the small and relatively constant 5d-moment. The 4f spin moment is spatially outside the core s-orbitals, but inside the valence s-orbitals. It will therefore induce exactly the opposite s-polarization on both of them⁶⁵.

Encouraged by the above observation that the m-orbitals of lanthanides in Fe yield identical orbital and dipolar fields as for free lanthanide ions, we now suppose that the ground state occupation of the 4f shell for lanthanides in Fe is the same Hund's rules ground state as for free lanthanide 3^+ ions.

For Tm^{3+} as an example, Hund's rules prescribe the orbitals with $m=+3$ and $m=+2$ for the 4f-up spin to be unoccupied, which yields from Fig. 6 and Fig. 7 the orbital and dipolar contributions listed in Tab. III. The Fermi contact field is almost independent on the orbital occupation, and is -39 T for Tm and all other lanthanides in Fe. The total HFF for the ground state of Tm in Fe – corresponding to a Tm^{3+} configuration – is hence $-745-53-39=-837$ T. This value is very close to what was found in a direct way in ‘case 1’ of Tab. I, a solution that has the same type of occupation as the Hund's rules ground state.

In this way, we can obtain by Fig. 6 an LDA+U orbital HFF for all lanthanides – in the antiferromagnetic type of solution – which is given by the full line in Fig. 3-a. In the same way, Fig. 7 leads to the LDA+U dipolar field, given by the full line in Fig. 3-b and Fig. 9 to the LDA+U Fermi field in Fig. 3-c. (It should be noted here that the core part from this calculated Fermi field most likely suffers from the typical ‘LDA core error’, for which recently a promising cure has been proposed⁶⁶.) The sum of all these contributions leads to an LDA+U value for the total HFF of all lanthanide 3^+ ions in Fe, which is

TABLE III: Contributions to B_{orb} , B_{dip} and V_{zz} for Tm in Fe in the Hund's rules ground state, using the information from figs. 6-8

Tm	$B_{orb}(T)$	$B_{dip}(T)$	$V_{zz}(10^{21}V/m^2)$
4f-up	-745	-49	-76.2
4f-down	-1	-1	0.9
5p-up	-84	10	16.1
5p-down	83	-13	21.2
6p-up	10	0	-0.7
6p-down	-8	0	0.1
Sum	-745	-53	-38.6

given by the full line in Fig. 1-b. The agreement with experiment is rather good for many lanthanides, especially in the middle of the series. Towards the beginning and the end, there is moderate disagreement. Only for Yb there is a large deviation between an accurate and reliable experimental value of -125 T (TDPAC) and a calculated value for the 3^+ ion of -570 T. Yb, however, often occurs in a divalent configuration, where the 4f shell is completely filled. This results in the -39 T of the Fermi contact field only, which is in much better agreement with experiment. Nevertheless, a trivalent configuration was suggested before⁴², from the following experimental considerations: the -125 T for Yb in Fe was considered to be 'large', much larger than the (-)61 T for the divalent Lu in Fe. This additional -64 T was taken as stemming from an orbital contribution, which must lead to the conclusion that the Yb is trivalent. From Fig. 1-a, however, we see that such a difference of 64 T is almost negligible, and that the expected orbital contribution for a trivalent state would be 10 times larger. The HFF for the other lanthanides in a divalent configuration is shown in Fig. 1-b as well (dashed line). Although the agreement is better now for Er and Tm, the uncertainty on the calculated values is too large to pretend that they would be divalent as well (which is for Er extremely unlikely, anyway). Another lanthanide that is often divalent is Eu. The experimental HFF lies halfway between the HFF for Eu^{2+} and Eu^{3+} , such that at this stage no definite conclusion on the valency is possible yet. Mössbauer isomer shift data^{48,49}, however, convincingly point to trivalency for Eu in Fe (see Sec. IV B for a continuation of this discussion and a final conclusion on the Eu valency). Irrespective of the valence configuration we consider, one can see that a moderate deviation from experiment for La, Ce and Pr still remains for the LDA+U calculations. The LDA results are closer to experiment. As was mentioned in Sec. I, LDA calculations for lanthanides represent an itinerant (also called delocalized) 4f configuration, which is mostly not what is found in Nature: the radius of the 4f orbitals is not very large, overlap with the orbitals of neighboring atoms is negligible, and as a result the 4f orbitals are localized. The only exception is Ce. As the

4f radius gets smaller for increasing atomic number Z , the 4f orbitals of Ce reach most outwards. The radius is just large enough to allow overlap and hence delocalization in materials where the nearest neighbor distance is not too large. Therefore, Ce can be either trivalent or itinerant, depending on the material^{63,67}. One can say that in the lanthanide series there is a delocalization-localization transition, that happens already at the very first element, Ce. The good agreement between experiments and the LDA-results up to Pr in Fig. 1-b, suggests that not only Ce but also Pr has delocalized 4f electrons in an Fe host: a 'postponed' delocalization-localization transition. Three additional arguments support this hypothesis. The first one is given in Fig. 10, where for all lanthanides in Fe the number of electrons inside the muffin tin sphere with radius $R_{mt} = 2.45$ a.u. is plot for the 3 most occupied m -orbitals in the unfilled spin channel, and compared with the average number of electrons in the same muffin tin sphere for occupied orbitals in the free lanthanide ions (which is almost unity). All data are for LDA+U calculations. Even though LDA+U favors localization, one can see that the occupation of the orbitals for Ce and Pr is far from 1: the 4f electrons are distributed in noninteger quantities over all 7 m -orbitals and/or reach out of the muffin tin sphere. This is a signature of delocalized behavior. (Two notes: 1. our procedure to extract the contributions for a single orbital works even with such noninteger occupations as input. The LDA+U values in Figs. 1-b and 11 are therefore really values for localized orbitals, although this localization is not realized in the LDA+U calculations themselves; 2. Fig. 10 should not be considered as a proof that from Nd on the 4f electrons are localized. These are results from LDA+U, which favors localization. Even LDA+U is not able to localize the 4f up to Pr. Therefore fig. 10 offer a lower bound for the delocalization transition (delocalization *at least* up to Pr). It does not exclude that, in Nature, Nd, Pm,... in Fe could be delocalized as well.) A second supporting argument comes from the lanthanide-Fe distance: 2.60 Å, which is considerably smaller than a typical lanthanide-lanthanide distance in pure lanthanide metals (4.08 Å). One can expect from this a large overlap between the 4f orbitals and the Fe-3d, and hence a stronger tendency to delocalization. This argument will be further quantified in terms of pressure in Sec. V A. Finally, in Sec. IV B, we will show that also the EFG of Ce in Fe indicates delocalized 4f behavior. In conclusion, we can say that there are several strong indications that the delocalization-localization transitions for lanthanides in Fe is somewhat postponed, at least up to Pr. We will come back to this in Sec. V A.

Regardless of the ambiguity to choose between divalent and trivalent configurations, one conclusion can be made unambiguously from Fig. 1-b: the magnitudes of the HFF's with LDA+U are much closer to experiment than with LDA, certainly for the heavier lanthanides. Together with the antiferromagnetic coupling which is reproduced by LDA+U but not everywhere by LDA

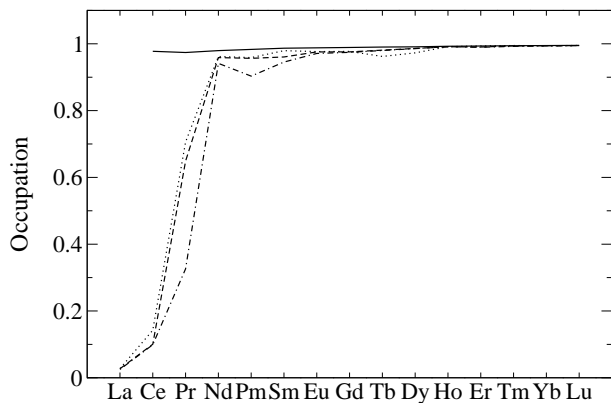


FIG. 10: The average occupation of the m -orbitals for the free ions (full line) compared with the occupation of the 3 orbitals in the unfilled spin-channel that are most occupied for lanthanide in Fe (dotted, dashed and dotted-dashed lines)

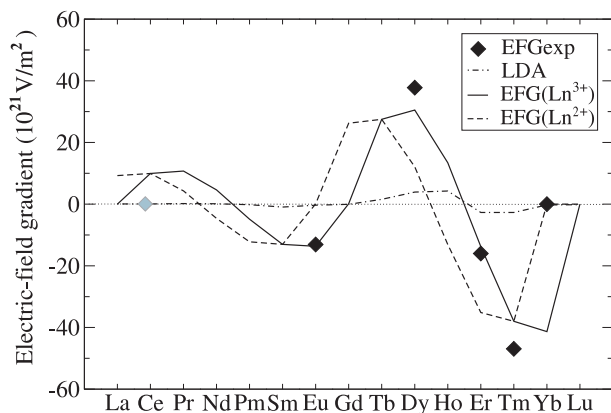


FIG. 11: V_{zz} for lanthanides in Fe. Symbols: experimental data^{12,42,49,68} (see text). The gray symbol for Ce indicates that this value is a – rather safe – guess (see text). Dotted-dashed line: LDA results. Full line: LDA+U values for trivalent lanthanides (using the information of Fig. 8, see text). Dashed line: LDA+U values for divalent lanthanides.

(Fig. 4), this is hard evidence for the fact that LDA+U performs considerably better than LDA also in these systems.

IV. ELECTRIC-FIELD GRADIENTS

A. Experimental data set

Only few experimental data on the main component V_{zz} of the electric-field gradient tensor for lanthanides in Fe are available (Fig. 11). For Eu, Dy, Er and Tm, Mössbauer measurements^{12,49} were done. Some attention is needed for Eu, which is reported to have $V_{zz} = 0$ in Ref. 12, based on ¹⁵¹Eu Mössbauer spec-

troscopy from Ref. 48. Niesen and Ofer, however, have later shown⁴⁹ by ¹⁵³Eu Mössbauer spectroscopy that $V_{zz} = -11.1 \cdot 10^{21} \text{ V/m}^2$. For Ce in Fe the quadrupole coupling constant (which contains the product between V_{zz} and the quadrupole moment Q) has been determined by ¹⁴¹Ce NMR⁶⁸ to be almost zero. The quadrupole moment for ¹⁴¹Ce is not known, but assuming a typical value of 1 barn leads to a V_{zz} that is practically zero (gray symbol in Fig. 11). The zero V_{zz} for Yb is not explicitly mentioned in the literature, but can be inferred from Fig. 1 in Ref. 42, which shows a purely magnetic interaction.

B. LDA+U calculations

As in an LDA-calculation all f -orbitals are roughly equally populated, there is almost no spatial anisotropy and V_{zz} will be close to zero (dotted-dashed line in Fig. 11). We therefore turn immediately to LDA+U calculations. We are confronted with the same problems as described in Sec. III C – V_{zz} sensitively depends on the f -electron density matrix and there is no criterion to determine which density matrix corresponds to the ground state – and therefore we determine again the individual contribution to V_{zz} of every 4f m -orbital and the induced 5p contributions to V_{zz} (Fig. 8 and Tab. II). Just as for the dipolar HFF, the EFG due to the 4f orbitals themselves does not depend on the direction of motion of the electron, and $\pm m$ -orbitals yield the same V_{zz} . On the other hand, the EFG depends on the charge and not on the spin, such that also up and down 4f-electrons yield the same V_{zz} . The 5p contribution depends on the 4f occupation, just as for the dipolar HFF. Assuming a Hund’s rules type of occupation either for divalent or trivalent ions, leads to reasonable agreement with experiment (Fig. 11). Fig. 11 provides further evidence for the fact that Yb in Fe really is divalent: trivalent Yb has a very large V_{zz} , while the experimental value is zero, in agreement with the divalent prediction. For Eu, the measured negative V_{zz} is in good agreement with the calculated value for a trivalent state. Together with the experimental evidence based on the isomer shift (Sec. III C), we can now firmly conclude that Eu in Fe is indeed trivalent, and has a valence state which is different from the one of Yb. For Er, Fig. 11 suggests trivalency as well, a conclusion that could not be unambiguously made based on the HFF only (Sec. III C). For Tm, the situation remains undecided. Irrespectively of the valence state we consider for Ce, a large deviation from experiment can be observed. However, the experiment matches very well with the itinerant LDA result. This is another indication that Ce in Fe has delocalized f -electron.

Now we can analyze which are the main electrons that provide the anisotropy that leads to the EFG. It has been shown before⁶⁹ in a rigorous way that for metals with s -, p - and d -electrons the total V_{zz} can be obtained as a sum of a quantity V_{zz}^{p-p} and V_{zz}^{d-d} (neglecting small

TABLE IV: Contributions to V_{zz} for Tb in Fe, with the down-channel for Tb-4f completely filled and with for the 4f-up channel one electron in the $m=-1$ orbital. The first column gives the rigorous notation of each contribution (see Ref. 69). In the second column an interpretative notation is defined, that is used in the text and in Fig. 8. The third column gives the energy region in the Density Of States (DOS) near to which these states are found (E_F means “near the Fermi energy”, negative values are below the Fermi energy). Units: 10^{21} V/m².

		in DOS (eV)	up	down	
V_{zz}^{d-d} (5d)	V_{zz}^{5d}	E_F	0.1	0.4	
V_{zz}^{p-p} (5p)	V_{zz}^{5p}	-23	5.6	9.6	
V_{zz}^{p-p} (6p)	V_{zz}^{6p}	E_F	-0.2	0.4	
V_{zz}^{f-f} (4f)	V_{zz}^{4f}	-5	-29.0	2.5	
V_{zz}			-23.5	12.9	sum = -10.6

contributions from the interstitial region of the crystal). They measure the nonspherical p and d charge densities $\rho_{20}^{p-p}(r)$ and $\rho_{20}^{d-d}(r)$, respectively, weighted by an integral over $1/r^3$:

$$V_{zz}^{p-p} \propto \int_0^R \frac{\rho_{20}^{p-p}}{r^3} dr \quad (1)$$

$$V_{zz}^{d-d} \propto \int_0^R \frac{\rho_{20}^{d-d}}{r^3} dr \quad (2)$$

R is the radius of the muffin tin sphere of the considered atom. The factor $1/r^3$ strongly emphasizes the contribution from the region close to the nucleus, with small r . s-electrons do not contribute as they have spherical symmetry, and so-called ‘mixed’ s-d or s-p contributions are negligible and therefor omitted. This can be extended to materials with f-electrons, such that V_{zz} for lanthanides can be written as:

$$V_{zz} \approx V_{zz}^{p-p} + V_{zz}^{d-d} + V_{zz}^{f-f} \quad (3)$$

We now apply this analysis to Tb in Fe, which is a particularly clear example because all 4f-down orbitals are fully occupied and there is only a single 4f-up electron. Tab. IV shows the different contributions to V_{zz} when this single electron is put in the $m=-1$ (up) orbital (this is not the ground state, but this is just an example, anyway). Tab. IV shows that the main contribution to the total $V_{zz} = -10.6 \cdot 10^{21}$ V/m² is due to the single 4f-up electron: $V_{zz}^{4f} = -29.0$. There is a large contribution of $5.6+9.6=15.2$ with the opposite sign due to p-electrons. What is surprising is that this p-contribution does not stem from the valence 6p electrons, but from the entirely filled and strongly bound 5p shell, which lies more than 20 eV below the Fermi energy. Intuitively, one would have assumed such a filled and well-bound shell to be entirely spherically symmetric, which would mean $V_{zz}^{5p} = 0$. And indeed, the 5p-anisotropy $\Delta p = \frac{1}{2} (n_{p_x} + n_{p_y}) - n_{p_z}$

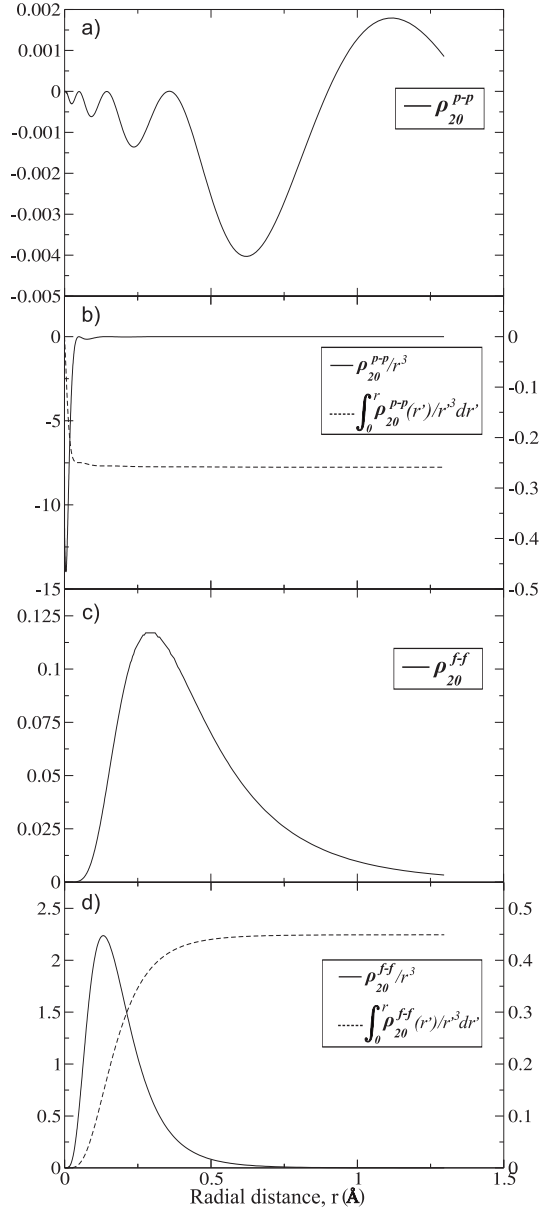


FIG. 12: a) The anisotropic p-density $\rho_{20}^{p-p}(r)$ for Tb in Fe (sum of up and down electrons, arbitrary units for y-scale). b) Left axis (arbitrary units): $\rho_{20}^{p-p}(r)/r^3$ for Tb in Fe. Right axis (arbitrary units): integral of $\rho_{20}^{p-p}(r)/r^3$, which is called V_{zz}^{p-p} (apart from a constant factor with negative sign). c) and d): idem, but for the f-f contribution.

is very small: 0.0030 (up) and 0.0040 (down) (it is shown in Ref. 69 that Δp is proportional to V_{zz}^{5p} ; n_{p_i} is the number of electrons in the p_i orbital, and Δp measures the unequal occupation of the 3 p-orbitals). However, a considerable part of this anisotropy stems from a region very close to the nucleus and hence gets amplified by the $1/r^3$ factor. This is demonstrated in Fig. 12, where for the same Tb-configuration the bare anisotropic p-p charge density $\rho_{20}^{p-p}(r)$ is shown, before (Fig. 12-a) and

after (Fig. 12-b) weighing with a $1/r^3$ factor, and also after integration (Fig. 12-b, right axis). Figs. 12-c and 12-d repeat this for the f-f contribution. The final integrals are clearly determined exclusively by anisotropies in a region closer than 0.05 \AA to the nucleus. In the expression for a spin dipolar field, the same factor $1/r^3$ is present, explaining why a similar dependence of the 5p dipolar field on the 4f occupation was observed there (Fig. 7-c,d,e).

A generalization of this analysis is given in Fig. 8, which shows the same individual 4f m-orbital contributions to V_{zz} for lanthanides split into 4f and 5p (i.e. when a given 4f m-orbital is occupied, Fig. 8-a,b shows the direct contribution from this orbital, while Fig. 8-e shows the corresponding induced contribution of the 5p-shell (up and down summed)). This shows that the opposite signs for 5p and 4f as seen in the example of Tb is a general effect: occupying the 4f $m=0$ orbital gives a negative direct 4f contribution but induces a positive 5p contribution, etc. This can be understood as follows. A negative V_{zz} corresponds to charge accumulation along the z-axis, a positive V_{zz} to charge accumulation in the xy-plane. The shape of the 4f orbitals is such that $m=0$ has its charge mainly along the z-axis (reflected in a negative V_{zz}^{4f}), while the xy-plane is more and more occupied for larger $|m|$. Apparently the 4f electrons dispel the 5p electrons: if $m=0$ is occupied, then the 5p electrons are forced away from the z-axis into the xy-plane, resulting in a positive V_{zz}^{5p} and Δp . As Tab. IV shows, a 4f-up electron distorts the 5p orbitals with either spin: this is an interaction between the electron charges, not between the spins.

Recently, the EFG of the actinide U has been analyzed in UO_2 by R. Laskowski et al. (Ref. 70), using the same APW+lo method as used in this work. These authors show in their Fig. 2 the contributions of V_{zz}^{p-p} , V_{zz}^{d-d} and V_{zz}^{f-f} as a function of the deformation of the oxygen cage that surrounds the U atom. They do not further divide the p-p contribution in 6p and 7p (here the 6p shell is entirely filled and well-bound). Without deformation of the oxygen cage, the crystallographic surrounding is cubic and the slightly non-zero $V_{zz} \approx -2 \cdot 10^{21} \text{ V/m}^2$ is due to spin-orbit coupling only, as is the case for lanthanides in Fe (compare with Nd in Fig. 11). This small V_{zz} is a sum of a f-f contribution of +20 and a p-p contribution of -21 (the d-d contribution is small: -1). This can be compared to Fig. 8 for Nd with the $m=(-3, -2, -1)$ orbitals filled, which leads to a 4f-contribution +14 and a 5p-contribution of -12, quite similar values. Because of this analogy, we suggest that also for U in UO_2 the p-p contribution for an undistorted oxygen cage is due to the completely filled 6p shell. This interpretation would furthermore imply that as a function of oxygen cage deformation, the 6p-contribution in Fig. 2 of Ref. 70 would remain almost constant (just as the 5f-contribution does), and that the strong decrease of the total p-p contribution is due to 7p only. This makes sense, as this decrease is attributed⁷⁰ to the tails of the O-2p wave functions, and hence should appear near the Fermi energy (= the region

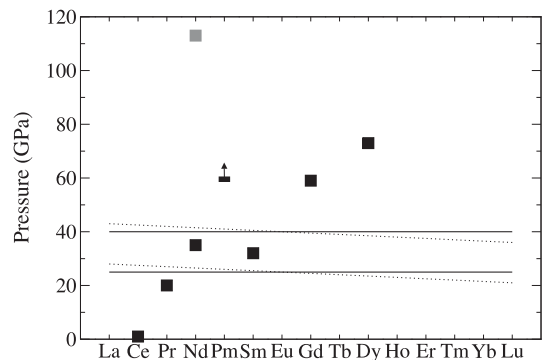


FIG. 13: The experimental transition pressure from localized 4f to delocalized 4f electrons for pure lanthanides (squares) and two possible choices for the effective pressure felt by lanthanides in Fe (full and dotted lines) (for details see text)

of the 7p).

V. ELABORATIONS

A. Pressure

It is well known experimentally⁷¹ that the pure lanthanides exhibit a large variety of structural phase transitions as a function of external pressure. At certain pressures, volume collapses are sometimes observed and attributed to the delocalization of the f electrons. These delocalization pressures have been determined for 6 elements of the lanthanide series: Ce^{72,73}, Pr^{74,75,76,77}, Nd^{78,79,80}, Sm^{78,81,82}, Gd⁷¹ and Dy⁸³ (Fig. 13). For Ce the delocalization of the f electrons occurs around the pressure of 1 GPa and is accompanied by a volume collapse of 16% at the isostructural transition to another fcc phase (α -Ce). Pr transforms to a α -U structure at 20 GPa with a volume collapse of 9-12%. In Gd 4f delocalization occurs at 59 GPa when the structure changes to body-centered monoclinic (bcm) with a volume collapse of 10.6% and in Dy this happens at 73 GPa with a volume collapse of 6%. For Nd and Sm no volume collapse has been observed. In these two cases the delocalization of the 4f electrons was associated with the appearance of low-symmetry structures (similar with those that appear in Pr, Gd and Dy cases with volume collapse). This is a somewhat ambiguous procedure. For Nd two transition pressures have been proposed: 40 GPa (corresponding to the transition to an hP3 structure^{78,79}) and 113 GPa (corresponding to the transition to the α -U phase⁸⁰). For Sm the delocalization pressure is proposed to be 37 GPa, when the Sm structure changes to hP3. For Pm we have only a lower limit for the transition pressure, 60 GPa (until this pressure no low-symmetry structure has been observed⁸⁴). In our calculations for lanthanide impurities we replace an Fe atom from an iron

lattice by a lanthanide atom. Obviously the lanthanide atom (which has a much larger volume) will feel a chemical pressure or effective pressure. How large will this effective pressure be? We concluded in Sec. III C that at least Ce and Pr are delocalized. Hence, the effective pressure – which we assume to be independent on the lanthanide in a first approximation – should be at least 20 GPa (Fig. 13). The hyperfine fields for Nd and Sm are only very approximately measured (Fig. 1-a), such that one cannot conclude whether they are localized or not. Based on isomer shift and EFG (Fig. 11), Eu is definitely localized, as are all heavier lanthanides. Therefore, two qualitatively different proposals for the effective pressure are possible: about 25 GPa (everything starting with Nd is localized) or about 40 GPa (everything below Eu is delocalized, except for Pm and maybe Nd). Assuming an effective pressure that is not constant (motivated by the decreasing volume of heavier lanthanides) does not change this picture (dotted lines in Fig. 13 – these lines qualitatively take the lanthanide contraction into account). A more accurate experimental determination of HFF and EFG for Nd, Pm and Sm in Fe would allow to distinguish between both scenarios and would allow to determine the real position of the delocalization-localization transition in this system. Experimental data for Nd in Fe are also for another reason interesting: if Nd in Fe would be found to be localized (itinerant) and the effective pressure of 40 GPa would known to be correct (from a Sm-measurement for instance) than the delocalization pressure of 113 GPa (35 GPa) for bulk Nd is probably correct. If the effective pressure of 25 GPa would be correct, no such conclusion can be made.

In conclusion for this section, accurate measurement of HFF and EFG for Nd, Pm or Sm in Fe would offer a lot of information.

B. Free lanthanide ions

LDA+U calculations for free lanthanide 3^+ ions were already mentioned in Figs. 5- 8. A quite complete experimental data set exists for this situation as well, both for the HFF (Fig. 14-a) and the EFG (Fig. 14-b) (data are copied from Ref. 85, the original data are in Ref. 86). In the experiments, the ions were not really free but were incorporated in a paramagnetic salt, and the effect of crystal fields was removed later in order to find the free ion values. By the same procedure as explained for lanthanides in Fe, we extracted LDA+U predictions for the HFF and V_{zz} for divalent and trivalent lanthanide ions, which are given by dashed and full lines in Fig. 14, respectively. For lanthanides in Fe, the positive z-direction was naturally defined by the moments of the ferromagnetic Fe host atoms. For free lanthanides, the total (=spin+orbital) angular momentum J determines the positive z-direction. Due to this different choice of axes, there is an *apparent* sign change for the heavy lanthanides between Fig. 1 (in Fe) and Fig. 14-a (free). The agree-

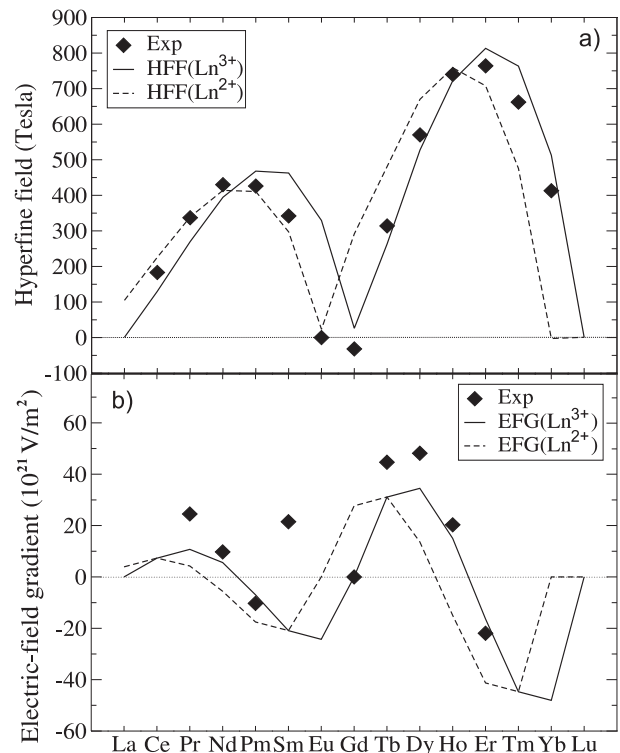


FIG. 14: a) Experimental value for the HFF in free lanthanide ions, compared with LDA+U predictions based on Figs. 6, 7 and 9, both for divalent and trivalent lanthanides. b) Experimental value for V_{zz} in free lanthanide ions, compared with LDA+U predictions based on Fig. 8, both for divalent and trivalent lanthanides.

ment with experiment is again quite nice. Eu is divalent (it was trivalent in Fe), while Yb is trivalent (it was divalent in Fe). For Sm there is a large deviation, both for the HFF and V_{zz} . But this is no surprise: it is well-known there are low-lying excited states in Sm which will mix with the ground state, such that our procedure which is based on Hund’s rules ground states is expected to fail.

C. Non-collinear Magnetism

The possibility to consider non-collinear magnetism at every infinitesimal region of space has recently been implemented⁷⁰ in the WIEN2k code. In principal this can be an important feature even for collinear antiferromagnets as we are dealing with here: it allows the spin moment to turn *gradually* from the Fe-orientation to the opposite lanthanide-orientation, and this is a better replication of what happens also in nature. We did not attempt a full study, but calculated HFF and EFG for Tm in Fe only. All technical parameters were chosen exactly the same as in the collinear calculations. For Tm in Fe as test example, the total HFF changes from -822 T in the collinear LDA+U calculation to -838 T in a non-collinear one, while the EFG remains exactly the same: $-38.1 \cdot 10^{21}$

V/m². Such a change of 16 T is not small in absolute value, but is negligible compared to the large values of the HFF's in this problem. Therefore we conclude that non-collinear magnetism doesn't play an important role for lanthanides in Fe.

VI. CONCLUSIONS AND OUTLOOK

We have demonstrated that LDA leads to a qualitatively wrong behavior for the magnetism of lanthanides in Fe. Using LDA+U, qualitative and quite reasonable quantitative agreement with experiment is obtained, both for HFF and EFG. This shows that the semi *ab initio* LDA+U method is a useful tool even for such sensitive quantities as hyperfine parameters of strongly correlated impurities in an itinerant magnetic host. We could come to these conclusions only after applying a careful strategy in order to cope with the lack of a good criterion to determine the true ground state if LDA+U is used. For all lanthanides the 4f spin moment couples antiferromagnetically to the Fe 3d moment, in agreement with the model of Campbell and Brooks. The orbital HFF is by far the dominant contribution to the total HFF (Figs. 1 and 3). The calculated value of the EFG for lanthanides in Fe agrees well with the few experimental data (Fig. 11). We discovered an unexpectedly strong contribution of the completely filled 5p shell to the dipolar HFF and the EFG, which can be explained by their common $1/r^3$ dependence: small deformations of the 5p shell in a region close to the nucleus are strongly emphasized. A reinterpretation of recent EFG calculations⁷⁰ for Uranium in UO₂ suggests that the same is true for the 6p shell in actinides. Furthermore, we conclude that Yb is divalent in an Fe host, while all other lanthanides are trivalent (including Eu, with perhaps an exception for Tm). The lightest lanthanides (at least up to Pr) show delocalized 4f behavior, and we conclude that the delocalization-localization transition that typically happens already at Ce is postponed for lanthanides in Fe: it falls at least after Pr and current experiments do not exclude that it could go up to Sm (although Pm is certainly localized). This can be explained by the large effective pressure that is felt by these lanthanide impurities (either 25 or 40 GPa - Fig. 13), leading to a larger overlap between the 4f wave functions and the neighboring Fe-3d. The question of a postponed localization transition has never been touched before in the 40 years of experiments on this system. This illustrates what can be the added value of *ab-initio* calculations for hyperfine interactions studies. Also in the case of free lanthanide ions, HFF and EFG can be quantitatively reproduced. Remarkably, Eu is divalent in this case and Yb is trivalent

– just the opposite as for lanthanides in Fe. The effect of fully non-collinear magnetism on this problem was tested to be negligible.

Obviously, the numerical agreement of the calculated hyperfine fields with experiment is for these lanthanides still much less satisfactorily than it is for lighter impurities. With the current methods, there are only limited possibilities to improve the accuracy of the calculations. The supercell can be extended to e.g. 32 atoms and relaxation of the Fe-neighbours can be calculated for every individual element (this requires the calculation of forces including spin-orbit coupling and LDA+U, which is time-consuming and not yet fully implemented in WIEN2k). But as inevitably a rather arbitrary choice remains to be made for the value of U , it is not clear whether these sophistications will really improve the agreement with experiment. And most likely they will not add anything new to the physical insight. In our opinion, new progress in this topic will have to come from experiment. Many of the experimentally determined HFF's and EFG's carry still large error bars. Accurate measurements – for instance with the NMR/ON method – are desirable (note that NMR/ON has not yet been applied for any of the lanthanides with a large EFG and/or HFF: such large hyperfine interactions put severe requirements on the equipment). The predicted HFF's and EFG's from this work should allow to reduce considerably the frequency domain that has to be scanned in an NMR/ON experiment, and warrants a more physical and reliable interpretation of the observed resonances. As most worthwhile experiments, we suggest a more accurate determination of HFF and EFG for Pr to Sm: this would allow to examine experimentally the position of the delocalization-localization transition. Once a data set with improved accuracy will be available, it can serve in its turn as a testing ground for future generations of *ab initio* many body methods.

Acknowledgments

Illuminating discussions with Th. Mazet (Nancy), P. Blaha (Vienna), P. Novák (Prague), M. Diviš (Prague), B. Barbara (Grenoble), N. Severijns (Leuven) and P. Schuurmans (SCK/CEN - Mol, Belgium) are gratefully acknowledged. The calculations were performed on a pc-cluster in Leuven, in the frame of projects G.0239.03 of the *Fonds voor Wetenschappelijk Onderzoek - Vlaanderen* (FWO), the Concerted Action of the KULeuven (GOA/2004/02) and the Inter-University Attraction Pole (IUAP P5/1). The authors are indebted to L. Verwilt and J. Knuts for their invaluable technical assistance concerning this pc-cluster.

* Electronic address: Stefaan.Cottenier@fys.kuleuven.ac.be

¹ G. Rao, *Hyperfine Interactions* **24-26**, 1119 (1985).

- ² H. Akai, M. Akai, S. Blügel, B. Drittler, H. Ebert, K. Terakura, R. Zeller, and P. H. Dederichs, *Prog. Theor. Phys. Suppl.* **101**, 11 (1990).
- ³ H. Haas, *Hyperfine Interactions* **151/152**, 173 (2003).
- ⁴ H. Akai, M. Akai, S. Blügel, R. Zeller, and P. H. Dederichs, *J. Magn. Magn. Materials* **45**, 291 (1984).
- ⁵ M. Akai, H. Akai, and J. Kanamori, *J. Phys. Soc. Japan* **54**, 4246 (1985).
- ⁶ H. Akai, M. Akai, and J. Kanamori, *J. Phys. Soc. Japan* **54**, 4257 (1985).
- ⁷ T. Korhonen, A. Settels, N. Papanikolaou, R. Zeller, and P. H. Dederichs, *Phys. Rev. B* **62**, 452 (2000).
- ⁸ S. Cottenier and H. Haas, *Phys. Rev. B* **62**, 461 (2000).
- ⁹ H. Ebert, R. Zeller, B. Drittler, and P. H. Dederichs, *J. Appl. Physics* **67**, 4576 (1990).
- ¹⁰ M. Akai, H. Akai, and J. Kanamori, *J. Phys. Soc. Japan* **56**, 1064 (1987).
- ¹¹ M. Takeda, H. Akai, and J. Kanamori, *Hyperfine Interactions* **78**, 383 (1993).
- ¹² L. Niesen, *Hyperfine Interactions* **2**, 15 (1976).
- ¹³ A. L. de Oliveira, N. A. de Oliveira, and A. Troper, *J. Phys.: Condensed Matter* **14**, 1949 (2002).
- ¹⁴ M. Richter, *J. Phys. D: Appl. Phys.* **31**, 1017 (1998).
- ¹⁵ M. Diviš, K. Schwarz, P. Blaha, G. Hilscher, H. Michor, and S. Khmelevskiy, *Phys. Rev. B* **62**, 6774 (2000).
- ¹⁶ L. Petit, A. Svane, Z. Szotek, P. Strange, H. Winer, and W. M. Temmerman, *J. Phys.: Condensed Matter* **13**, 8697 (2001).
- ¹⁷ S. J. Asadabadi, S. Cottenier, H. Akbarzadeh, R. Saki, and M. Rots, *Phys. Rev. B* **66**, 195103 (2002).
- ¹⁸ V. I. Anisimov and O. Gunnarsson, *Phys. Rev. B* **43**, 7570 (1991).
- ¹⁹ M. T. Czyżyk and G. A. Sawatzky, *Phys. Rev. B* **49**, 14211 (1994).
- ²⁰ V. I. Anisimov, I. V. Solovyev, M. A. Korotin, M. T. Czyżyk, and G. A. Sawatzky, *Phys. Rev. B* **48**, 16929 (1993).
- ²¹ A. G. Petukhov, I. I. Mazin, L. Chioncel, and A. I. Lichtenstein, *Phys. Rev. B* **67**, 153106 (2003).
- ²² V. I. Anisimov, F. Aryasetiawan, and A. I. Lichtenstein, *J. Phys.: Condensed Matter* **9**, 767 (1997).
- ²³ V. N. Antonov, B. N. Harmon, and A. N. Yaresko, *Phys. Rev. B* **66**, 165208 (2002).
- ²⁴ R. Laskowski, P. Blaha, and K. Schwarz, *Phys. Rev. B* **67**, 075102 (2003).
- ²⁵ D. W. Boukhvalov, V. V. Dobrovitski, M. I. Katsnelson, A. I. Lichtenstein, B. N. Harmon, and P. Kogerler, *J. Appl. Physics* **93**, 7080 (2003).
- ²⁶ A. B. Shick and O. N. Mryasov, *Phys. Rev. B* **67**, 172407 (2003).
- ²⁷ G. Seewald, E. Hagn, E. Zech, D. Forkel-Wirth, A. Burchard, and the ISOLDE Collaboration, *Phys. Rev. Letters* **78**, 1795 (1997).
- ²⁸ G. Seewald, E. Hagn, E. Zech, R. Kleyna, M. Voss, D. Forkel-Wirth, A. Burchard, and the ISOLDE Collaboration, *Phys. Rev. Letters* **82**, 1024 (1999).
- ²⁹ G. Seewald, E. Hagn, E. Zech, R. Kleyna, M. Voss, A. Burchard, and the ISOLDE Collaboration, *Phys. Rev. B* **66**, 174401 (2002).
- ³⁰ P. Hohenberg and W. Kohn, *Phys. Rev.* **136**, 864 (1964).
- ³¹ W. Kohn and L. J. Sham, *Phys. Rev.* **140**, A1133 (1965).
- ³² S. Cottenier, *Density Functional Theory and the Family of (L)APW-methods: a step-by-step introduction*, (Instituut voor Kern- en Stralingsfysica, KULeuven, Belgium) (2002), ISBN 90-807215-1-4 (to be found at http://www.wien2k.at/reg_user/textbooks).
- ³³ E. Sjöstedt, L. Nordström, and D. J. Singh, *Solid State Commun.* **114**, 15 (2000).
- ³⁴ G. K. H. Madsen, P. Blaha, K. Schwarz, E. Sjöstedt, and L. Nordström, *Phys. Rev. B* **64**, 195134 (2001).
- ³⁵ P. Blaha, K. Schwarz, G. Madsen, D. Kvasnicka, and J. Luitz, *WIEN2k, An Augmented Plane Wave + Local Orbitals Program for Calculating Crystal Properties*, (Karlheinz Schwarz, Techn. Universität Wien, Austria) (1999), ISBN 3-9501031-1-2.
- ³⁶ J. P. Perdew and Y. Wang, *Phys. Rev. B* **45**, 13244 (1992).
- ³⁷ D. D. Koelling and B. N. Harmon, *J. Phys. C* **10**, 3107 (1977).
- ³⁸ J. Kuneš, P. Novák, R. Schmid, P. Blaha, and K. Schwarz, *Phys. Rev. B* **64**, 153102 (2001).
- ³⁹ J. Goto, M. Tanigaki, A. Taniguchi, Y. Ohkubo, Y. Kawase, S. Ohya, K. Nishimura, T. Ohtsubo, and S. Muto, *J. Phys. Soc. Japan* **15/16**, 325 (1983).
- ⁴⁰ W. van Rijswijk, F. van den Berg, W. Joosten, and W. Huiskamp, *Hyperfine Interactions* **15/16**, 325 (1983).
- ⁴¹ P. Herzog, U. Dämmrich, K. Freitag, C.-D. Herrmann, and K. Schlösse, *Hyperfine Interactions* **22**, 167 (1985).
- ⁴² H. Devare, H. de Waard, and L. Niesen, *Hyperfine Interactions* **5**, 191 (1978).
- ⁴³ O. K. and H. Spehl and N. Wertz, *Z. Physik* **217**, 425 (1968).
- ⁴⁴ G. Russel, private communication to D.A. Shirley, cited in T.A. Koster and D.A. Shirley, *Proceedings of the International Conference on Hyperfine Interactions in Excited Nuclei*, Eds. G. Goldring and R. Kalish, Gordon and Breach Science Publishers, London (1971), p. 1239.
- ⁴⁵ F. Boehm, G. Hagemann, and A. Winther, *Phys. Letters* **21**, 217 (1966).
- ⁴⁶ L. Grodzins, R. Borchers, and G. Hagemann, *Phys. Letters* **21**, 214 (1966).
- ⁴⁷ R. Brenn, L. Lehmann, and H. Spehl, *Z. Physik* **209**, 197 (1968).
- ⁴⁸ R. Cohen, G. Beyer, and B. Deutch, *Phys. Rev. Letters* **33**, 518 (1974).
- ⁴⁹ L. Niesen and S. Ofer, *Hyperfine Interactions* **4**, 347 (1978).
- ⁵⁰ H. Wit, L. Niesen, and H. D. Waard, *Hyperfine Interactions* **5**, 233 (1978).
- ⁵¹ L. Niesen, P. Kikkert, and H. D. Waard, *Hyperfine Interactions* **3**, 109 (1977).
- ⁵² P. G. E. Reid, N. J. Stone, H. Bernas, D. Spanjaard, and I. Campbell, *Proc. Roy. Soc. (London)* **311**, 169 (1969).
- ⁵³ L. Niesen, Ph.D. thesis, University of Leiden (1971).
- ⁵⁴ H. W. Kugel, T. Polga, R. Kalish, and R. R. Borchers, in *Hyperfine Interactions in Excited Nuclei*, edited by G. Goldring and R. Kalish (Gordon and Breach, New York, 1971), p. 104.
- ⁵⁵ H. W. Kugel, L. Eytel, G. Hubler, and D. E. Murnick, *Phys. Rev. B* **13**, 3697 (1976).
- ⁵⁶ B. I. Deutch, G. B. Hagemann, K. A. Hagemann, and S. Ogaza, *Hyperfine Interactions (C)* p. 731 (1968).
- ⁵⁷ H. Bernas and H. Gabriel, *Phys. Rev. B* **7**, 268 (1973).
- ⁵⁸ I. Campbell, *J. Phys. F: Met. Phys.* **2**, L47 (1972).
- ⁵⁹ M. Brooks, O. Eriksson, and B. Johansson, *J. Phys.: Condensed Matter* **1**, 5861 (1989).
- ⁶⁰ E. Fermi, *Z. Physik* **60**, 320 (1930).
- ⁶¹ B. N. Harmon, V. Antropov, A. I. Lichtenstein, I. V. Solovyev, and V. I. Anisimov, *J. Phys. Chem. Solids* **56**, 1521 (1995).

- ⁶² J. F. Herbst, R. E. Watson, and J. W. Wilkins, *Phys. Rev. B* **17**, 3089 (1978).
- ⁶³ B. I. Min, H. Jansen, T. Oguchi, and A. J. Freeman, *J. Magn. Magn. Materials* **61**, 139 (1986).
- ⁶⁴ J. Bouchet, B. Siberchicot, F. Jollet, and A. Pasturel, *J. Phys.: Condensed Matter* **12**, 1723 (2000).
- ⁶⁵ R. E. Watson and A. J. Freeman, *Phys. Rev.* **123**, 2027 (1961).
- ⁶⁶ P. Novak, J. Kunes, W. E. Pickett, W. Ku, and F. R. Wagner, *Phys. Rev. B* **67**, 140403(R) (2003).
- ⁶⁷ J. L. Smith, Z. Fisk, and S. S. Hecker, *Physica* **130B**, 151 (1985).
- ⁶⁸ W. van Rijswijk, F. van den Berg, H. E. Keus, and W. J. Huiskamp, *Physica* **113B**, 127 (1982).
- ⁶⁹ P. Blaha, K. Schwarz, and P. H. Dederichs, *Phys. Rev. B* **37**, 2792 (1988).
- ⁷⁰ R. Laskowski, G. K. H. Madsen, P. Blaha, and K. Schwarz, *Phys. Rev. B* **69**, 140408(R) (2004).
- ⁷¹ A. K. McMahan, C. Huscroft, R. T. Scalettar, and E. L. Pollock, *Journal of Computer-Aided Materials Design* **5**, 131 (1998).
- ⁷² W. H. Zachariasen and F. H. Ellinger, *Acta Cryst. A* **33**, 155 (1977).
- ⁷³ J. S. Olsen, L. Gerward, U. Benedict, and J.-P. Itié, *Physica* **133B**, 129 (1985).
- ⁷⁴ G. S. Smith and J. Akella, *J. Appl. Physics* **53**, 9212 (1982).
- ⁷⁵ W. A. Grosshans, Y. K. Vohra, and W. B. Holzapfel, *J. Phys. F: Met. Phys.* **13**, L147 (1983).
- ⁷⁶ Y. C. Zhao, F. Porsch, and W. B. Holzapfel, *Phys. Rev. B* **52**, 134 (1995).
- ⁷⁷ B. J. Baer, H. Cynn, V. Iota, C.-S. Yoo, and G. Shen, *Phys. Rev. B* **67**, 134115 (2003).
- ⁷⁸ Y. C. Zhao, F. Porsch, and W. B. Holzapfel, *Phys. Rev. B* **50**, 6603 (1994).
- ⁷⁹ J. Akella, S. T. Weir, Y. K. Vohra, H. Prokop, S. A. Catledge, and G. N. Chesnut, *J. Phys.: Condensed Matter* **11**, 6515 (1999).
- ⁸⁰ G. N. Chesnut and Y. K. Vohra, *Phys. Rev. B* **61**, R3768 (2000).
- ⁸¹ W. A. Grosshans and W. B. Holzapfel, *J. Phys. (Paris)* **45**, 141 (1984).
- ⁸² J. S. Olsen, S. Steenstrup, L. Gerward, U. Benedict, J. Akella, and G. Smith, *High Press. Res.* **4**, 366 (1990).
- ⁸³ R. Patterson, C. K. Saw, and J. Akella, *J. Appl. Physics* **95**, 5443 (2004).
- ⁸⁴ R. G. Haire, S. Heathman, and U. Benedict, *High Press. Res.* **2**, 273 (1990).
- ⁸⁵ W. D. Brewer, *Hyperfine Interactions* **59**, 201 (1990).
- ⁸⁶ B. Bleaney, in *Magnetic Properties of the Rare-Earth Metals*, edited by R. Elliot (Plenum Press, London, 1972), p. 383.